Convection Compensated Electrophoretic NMR[1]

Qiuhong He[2] and Zhaohui Wei*

*Department of Chemistry, and *Department of Computer Science and Engineering, University of Connecticut, Storrs, Connecticut 06269*

A novel method of convection compensated ENMR (CC-ENMR) has been developed to detect electrophoretic motion of ionic species in the presence of bulk solution convection. This was accomplished using a gradient moment nulling technique to remove spectral artifacts from heat-induced convection and using the polarity switch of the applied electric field to retain spin phase modulations due to electrophoretic flow. Experiments were carried out with a mixture of 100 mM L-aspartic acid and 100 mM 4,9-dioxa-1,12-dodecanediamine to demonstrate this new method of ENMR. CC-ENMR enhances our previously developed capillary array ENMR (CA-ENMR) in solving the convection problem. The combined CA- and CC-ENMR approach strengthens the potential of multidimensional ENMR in simultaneous structural determination of coexisting proteins and protein conformations in biological buffer solutions of high ionic strength. Structural mapping of interacting proteins during biochemical reactions becomes possible in the future using ENMR techniques, which may have a profound impact on the understanding of biological events, including protein folding, genetic control, and signal transduction in general.   © 2001 Academic Press

Key Words: electrophoretic NMR; pulsed field gradient; flow and convection compensation; structure characterization of protein interactions.

INTRODUCTION

In a recent two-dimensional ENMR experiment, the one-dimensional NMR spectra of ubiquitin and bovine serum albumin (BSA) were distinguished without physical separation of the component proteins in D_2O solution (*1*). The experiment established the feasibility of separating multidimensional NMR spectra of coexisting proteins by their electrophoretic mobilities. In a subsequent three-dimensional electrophoretic COSY (EP-COSY) experiment, 2D COSY spectra of two molecules were obtained simultaneously in a solution mixture (*2*). The experiment revealed the potential of the new multidimensional electrophoretic NMR for structure determination of coexisting proteins and protein conformations and for structure characteri-

zation of protein interactions in solution. The technique enhances and refines conventional NMR methods that are employed to obtain spectra of proteins from single-component solutions for structure determination.

In the experiment of BSA and ubiquitin, a sample solution of low conductivity was prepared for electrophoretic flow measurements. The ENMR experiments using this protocol, however, failed for samples of high ionic strength due to insufficient electric field and heat-induced convection (*3*). The recent capillary array electrophoretic NMR (CA-ENMR) demonstrates a partial solution using bundled capillary array chambers (*3*). In CA-ENMR, the capillary walls block heat-induced convection, and the small cross-sectional areas of the capillary tubes enhance the effective electric field (*3*). As a result, protein electrophoretic oscillations can be detected in high-salt biological buffer solutions. We report here an alternative method of convection compensated electrophoretic NMR (CC-ENMR), which sensitizes electrophoretic motion in the presence of bulk convective flow. This is accomplished by using gradient moment nulling, a technique developed to eliminate flow artifacts in MRI (*4–7*), and by switching polarity of the applied DC electric field to generate electrophoretic signal modulations (*8–27*). The CC-ENMR experiments were conducted with a solution containing 100 mM L-aspartic acid and 100 mM 4,9-dioxa-1,12-dodecanediamine in D_2O. Electrophoretic interferograms were obtained with minimal convection artifacts, and the electrophoretic oscillation frequencies can be extracted to distinguish signals of different molecules migrating in solution in the presence of convection.

THEORY

The principle of CC-ENMR can be described using a two-level spin model. The theory holds true for multilevel coupled spin systems since the Hamiltonian governing spin dynamics commutes with the Hamiltonian governing the flow processes. In the rotating frame, the phase of a flowing spin isochromat, driven by both DC electric field and heat-induced convection, can be described as a function of the time-dependent gradient waveform, $\mathbf{G}(t)$, and the particle position, $\mathbf{r}(t)$:

$$\phi(t) = \gamma \int_0^t p(t)\mathbf{G}(t) \cdot \mathbf{r}(t)dt, \qquad [1]$$

---

[2] To whom correspondence should be addressed at Memorial Sloan-Kettering Cancer Center, Department of Medical Physics, 1275 York Avenue, New York, NY 10021. Fax: (212) 717-3676. E-mail: heq@mskcc.org.

where γ is the gyromagnetic ratio and $p(t)$ is the coherence order as a function of time (4–7). For spins migrating in the z-gradient direction, their spatial locations at time t can be expanded in term of their initial positions at $t = 0$ in the power series

$$z(t) = z_0 + \left[\frac{dz}{dt}\right]_{t=0} t + \frac{1}{2}\left[\frac{\partial^2 z}{\partial t^2}\right]_{t=0} t^2 + \cdots$$
$$+ \frac{1}{n!}\left[\frac{\partial^n z}{\partial t^n}\right]_{t=0} t^n + \cdots \qquad [2]$$

Each term contributes to the spin phase modulation as described by

$$
\begin{aligned}
\phi_0 &= \gamma z_0 m_0 \\
\phi_1 &= \gamma v_0 m_1 \\
\phi_2 &= \frac{\gamma}{2} a_0 m_2 \\
&\vdots \\
\phi_n &= \frac{\gamma}{n!}\frac{\partial^n z}{\partial t^n} m_n \\
&\vdots
\end{aligned}
\qquad , \qquad [3]
$$

where m_0, m_1, m_2, and m_n are the zeroth, first, second, and nth moments of magnetic field gradient with respect to time, t, respectively. The nth moment is defined by

$$m_n = \int_0^t p(t)G(t)t^n dt. \qquad [4]$$

Convection contributes to the higher-order terms of the gradient moments, including velocity (v_0), acceleration (a_0), and pulsatility, whereas the electrophoretic motion contributes to only the velocity term.

(i) Convection compensation. Pulsed field gradients are employed in ENMR experiments for spin refocusing and flow measurements (*1–3, 8–28*). The spin-echo formation requires that the zeroth gradient moment, m_0, be zero, whereas the electrophoretic flow measurement requires that the first gradient moment, m_1, be nonzero. The values of the higher-order terms of the gradient moments are nonzero in the presence of convection (and zero otherwise) (See Calculations). All previous ENMR sequences are prone to heat-induced convection, which could be detrimental to the investigations of proteins in biological buffer solutions of high ionic strength (*3*). Here we demonstrate that our CC-ENMR sequences can dramatically reduce convection artifacts in the ENMR spectra by employing gradient moment nulling techniques. A CC-ENMR sequence was constructed by
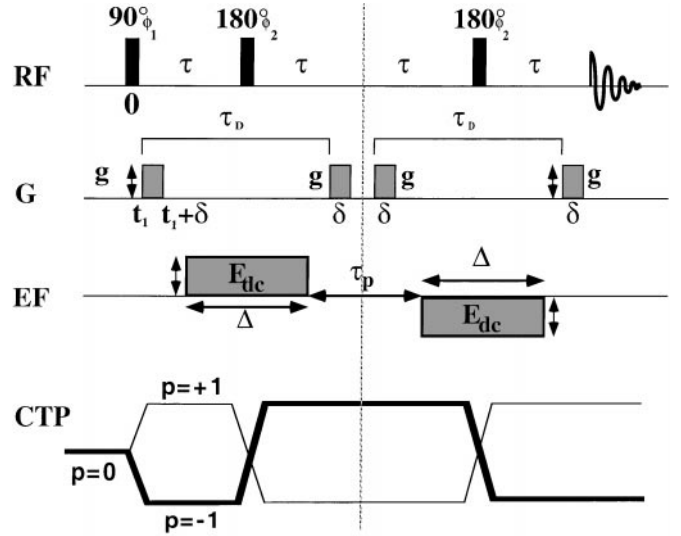
FIG. 1. The back-to-back spin-echo CC-ENMR pulse sequence and the coherence transfer pathways (CTP).

connecting back-to-back the two spin-echo ENMR sequences (Fig. 1). Because the coherence order, $p(t)$, has opposite signs in the two halves of the CC-ENMR sequence, the gradient moments change sign in the middle of the experiment. As a result, all order terms of the gradient moment are nulled: $m_k = 0$, where $k = 0, 1, 2, 3\ldots$ The convection-induced spin phase accumulation (Eq. 3) in the first half of the experiment ($\phi_{k,a}^c$) is refocused in the second half ($\phi_{k,b}^c$):

$$
\begin{aligned}
\phi_{k,a}^c &= \gamma v_0^c m_k^c \\
\phi_{k,b}^c &= \gamma v_0^c(-m_k^c), \\
\phi_{k,tot}^c &= \phi_{k,a}^c + \phi_{k,b}^c = 0,
\end{aligned}
\qquad [5]
$$

where the superscript "c" denotes convection and v_0^c the convective flow velocity.

(ii) Selective detection of electrophoretic flow. In CC-ENMR, the electrophoretic flow is selectively detected by switching polarity of the DC electric field between the two halves of the CC-ENMR sequence. The change of the ionic migrating direction cancels the phase-refocusing effect from the gradient moment nulling. Consequently, the phase accumulation of the transverse magnetization from the electrophoretic flow is
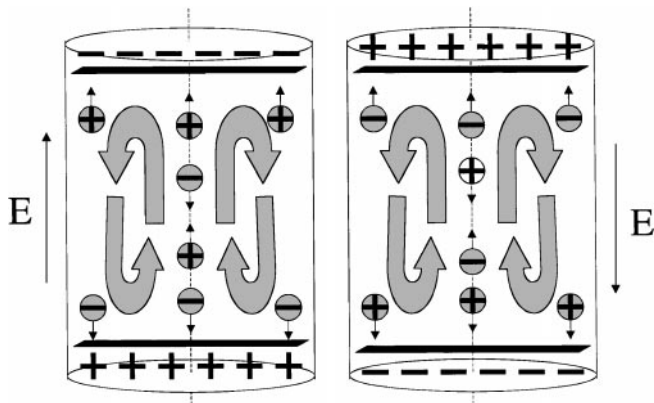
FIG. 2. Switching polarity of the electric field alters the electrophoretic flow direction (solid arrows); however, the procedure exerts no influence on the convective flow circulation (curled arrows).

maintained according to

$$
\begin{aligned}
\phi_{1,a}^{E} &= \gamma v_0^{E} m_1^{E} \\
\phi_{1,b}^{E} &= \gamma\left(-v_0^{E}\right)\left(-m_1^{E}\right), \\
\phi_{1,tot}^{E} &= \phi_{1,a}^{E} + \phi_{1,b}^{E} = 2\gamma v_0^{E} m_1^{E}
\end{aligned}
\tag{6}
$$

where the superscript "E" designates electrophoretic flow at the velocity, v_0^{E}. The polarity change of the electric field does not affect heat-induced convection, which originates from temperature gradient and gravitational forces. Gradient moment nulling remains effective to remove convection artifacts (Fig. 2).

The overall electrophoretic phase accumulation in CC-ENMR is twice that in each component of the spin-echo ENMR sequence blocks. For U-shaped ENMR sample chambers, the NMR signals are modulated by a cosine factor, $\cos(2K v_0^{E}\Delta)$ (8, 15):

$$
M(E_{dc}) = M(0)\exp\left[-2DK^2\left(\tau_D - \frac{\delta}{3}\right) - \frac{4\tau}{T_2}\right]
$$
$$
\times \cos[(2K E_{dc}\Delta)\mu],
\tag{7}
$$

as the strength of the electric field is increased, where $v_0^{E} = \mu E_{dc}$, $E_{dc} = \frac{I_e}{\kappa A}$, μ is the electrophoretic mobility, κ the conductivity of the solution, A the cross-sectional area of the electrophoretic tube, I_e the DC electric current, E_{dc} the amplitude, and Δ the duration of the electric field. The exponential decay factor comes from contributions of molecular diffusion and spin relaxation effects, where τ_D is the self-diffusion time, D is the molecular diffusion coefficient, T_2 is the spin–spin relaxation time, and $M(0)$ is the initial magnetization after the first 90° pulse.

CALCULATIONS

The spin phase accumulation from electrophoretic flow in the CC-ENMR sequence can be estimated from the first gradient moment, m_1, derived as

$$
\begin{aligned}
m_1 &= \int_0^{T=2\tau} p(t)G(t)t\,dt \\
&= \int_0^{t_1} g_0 t\,dt + \int_{t_1}^{t_1+\delta}(g_0+g)t\,dt + \int_{t_1+\delta}^{\tau} g_0 t\,dt \\
&\quad - \int_{\tau}^{t_1+\tau_D} g_0 t\,dt - \int_{t_1+\tau_D}^{t_1+\tau_D+\delta}(g_0+g)t\,dt - \int_{t_1+\tau_D+\delta}^{2\tau} g_0 t\,dt
\end{aligned}
\tag{8}
$$

in the first half of the CC-ENMR sequence using the time-dependent gradient waveforms,

$$
G(t) = \begin{cases}
g_0 & \begin{array}{l} 0 \le t < t_1; \\ t_1+\delta \le t < t_1+\tau_D > \tau; \\ t_1+\tau_D+\delta < t; \end{array} \\
g_0 + g & \begin{array}{l} t_1 \le t < t_1+\delta < \tau; \\ t_1+\tau_D \le t < t_1+\tau_D+\delta < 2\tau \end{array}
\end{cases}
\tag{9}
$$

and the coherence order,

$$
p(t) = \begin{cases}
1 & 0 \le t < \tau \\
-1 & \tau \le t < 2\tau,
\end{cases}
\tag{10}
$$

where g represents the amplitude and δ the duration of the applied gradient pulses, and g_0 is the amplitude of the background gradient from the magnetic field inhomogeneity. In most ENMR experiments where $g \gg g_0$ (i.e., g_0 is negligible), the first moment can be calculated as

$$
m_1^{E} = -g\delta\tau_D,
\tag{11}
$$

and the spin phase accumulation in the first half of the CC-ENMR sequence is

$$
\phi_{1,a}^{E} = \gamma v_0^{E} m_1^{E} = -K v_0^{E}\Delta,
\tag{12}
$$

where $K = \gamma g\delta$, and $v_0^{E} \neq 0$ only during the electric field pulse of duration $\Delta(\tau_D > \Delta)$. These results are consistent with our previous ENMR calculations (1, 3, 8–10, 12, 13, 15). The total spin phase accumulation in CC-ENMR from the electrophoretic flow,

$$
\phi_{1,T}^{E} = 2\phi_1^{E} = -2K v_0^{E}\Delta,
\tag{13}
$$

is twice that in each of the two spin-echo sequence components. In other words, the CC-ENMR has the same detection efficiency for electrophoretic flow measurements as the previous ENMR methods (*1–3, 8–10, 12, 13, 15, 23–25*). Similarly, the higher-order terms of the gradient moments $\{m_i$, where $i = 2, 3, \ldots, n\}$ are calculated to be nonzero for the conventional spin-echo sequence, indicating that the previous spin-echo ENMR approach is also susceptible to acceleration, pulsatility, and other modes of heat-induced convection. Since gradient moment nulling is achieved at all orders in CC-ENMR, the method removes all convection artifacts.

EXPERIMENTAL

All experiments were performed on a high-resolution Bruker AM 500 NMR spectrometer, using a commercial probe equipped with an actively shielded gradient in *z*-direction. A U-shaped 10-bundle capillary array ENMR sample cell was constructed from fused silica capillaries (ID = 250 μm, Chromasil, Spectran Corporation, Inc.). Two electrodes were housed in Teflon tube reservoirs at the end of the bundled capillary arms (*3*). In this configuration, bubbles generated by electrolysis on the two electrodes escaped without disturbing the sample solution in the receiver coil region. To prevent electroosmotic flow, the inner glass surfaces of the capillaries were treated with 1 M HCl, distilled water, and 1 M NaOH and coated with methylcellulose (Aldrich) following the treatment (*13*). The assembled CC-ENMR sample was introduced into a 5-mm NMR probe from the top of the magnet. No sample lifting or spinning air was used. The magnetic field gradient and the DC electric field pulses were generated from the electric field/gradient driver (Digital Specialties, Inc.). The electric field was produced in constant current mode with a maximum output voltage of 1 kV. The trigger pulses from the Bruker spectrometer, which was controlled from the CC-ENMR pulse sequence, defined the duration of the electric field pulse and the onset of the gradient pulses. The amplitudes of the electric field pulses, as well as the durations and amplitudes of the gradient pulses, were controlled by a PC 486 computer. The rising and falling time of the electric field was 1 ms/mA, whereas that of the gradient pulse was 10 μs. The polarity of the two electric field pulses was switched with an interpulse delay (τ_p) of 100 ms (Fig. 1). The experimental temperature of 25°C was maintained using cooling air supplied by the Bruker temperature control unit. The recorded ENMR spectra were processed on a Silicon Graphics Indigo2 workstation using Felix NMR software (Molecular Simulations, Inc.).

RESULTS

The effectiveness of CC-ENMR for convection compensation was assessed with a high-salt solution containing 100 mM L-aspartic acid (Acros) and 100 mM 4,9-dioxa-1,12-dodecanediamine (Aldrich) mixed in D_2O (99.9% atom %D, Aldrich). As the electric field was increased, convection ar-

tifacts grew progressively more pronounced in the control spin-echo ENMR experiment, as seen from the phase distortions of the water signal and from the signal decays of the ionic species (Fig. 3a). These convection artifacts are clearly reduced in the CC-ENMR spectrum (Fig. 3b), and the cosinusoidal electrophoretic signal oscillations of L-aspartic acid and 4,9-doxia-1,12-dodecanediamine become detectable. The electrophoretic mobilities of L-aspartic acid and 4,9-dioxa-1,12-dodecanediamine are calculated from the cosinusoidal oscillation frequencies of the CC-ENMR resonances as 2.98×10^{-4} and 2.76×10^{-4} cm^{2}V^{-1}s^{-1}, respectively. The resonances of the different molecules can be further displayed in the Fourier domain at different locations in the flow dimension (*1, 2, 8, 9, 24, 25*). This approach has been successfully applied to distinguish overlapping NMR resonances of different proteins in a solution mixture (*1*). In the conventional ENMR spectrum without convection compensation (Fig. 3a), these cosinusoidal oscillation characteristics are lost with convection artifacts preventing distinction of different ionic species.

The improved consinusoidal electrophoretic interferogram obtained in the CC-ENMR experiment validates the convection compensation strategy of using the combined gradient moment nulling and electric field switching. Under the present experimental conditions, the signal-to-noise ratio is slightly lower in CC-ENMR than in the conventional ENMR method (Figs. 3a and 3b). This may be partially due to imperfect 180° pulses for spin-echo refocusing and to the nonideal electric field pulses for convection compensation; however, most of the signal loss could be attributed to the convection pattern changes during the CC-ENMR experiment. Only spins experiencing the same convection circulation patterns in the two spin-echo sequence blocks would be refocused, whereas the dynamic change part of the convective flow pattern would not be compensated for in CC-ENMR. Obviously, the change of the convective circulation pattern during the long polarity switching time of the electric field pulse ($\sim$100 ms) was not refocused in the current experiment. Further removal of the convection artifacts may be possible by employing faster polarity-switching ENMR systems. However, the residual convection artifacts do not appear to have affected the experimental outcome.

DISCUSSIONS

A decade ago, He and Johnson and colleagues demonstrated two-dimensional (2D) ENMR (*8–10*). The work was followed by Morris and Johnson's mobility ordered electrophoretic NMR, which refined the flow resolution of 2D ENMR using linear prediction and cylindrical ENMR sample chambers (*24, 25*). These early 2D ENMR methods, however, cannot be applied to protein investigations in biological buffer solutions of high ionic strength because the electric field ($E_{dc} = \frac{I_e}{\kappa A}$) decreases substantially for electrolyte solutions of high conductivity (κ). A relatively large electric current is required to establish sufficient electric field for ENMR measurements in these solutions.
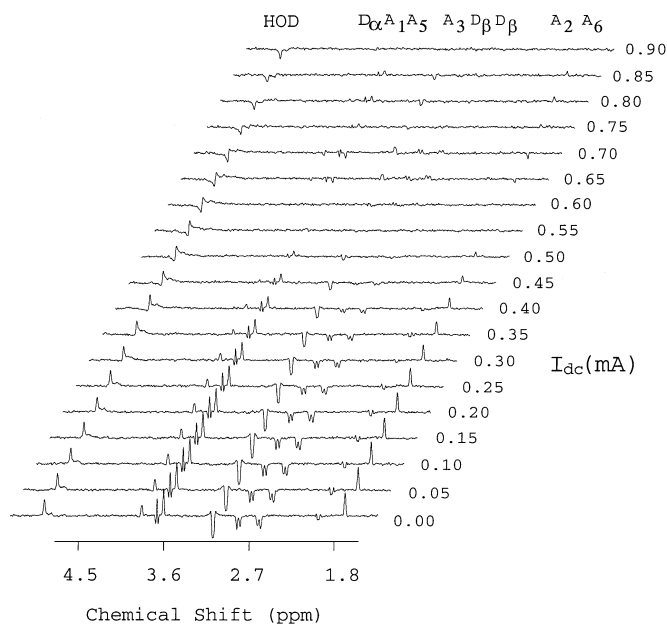
(a)
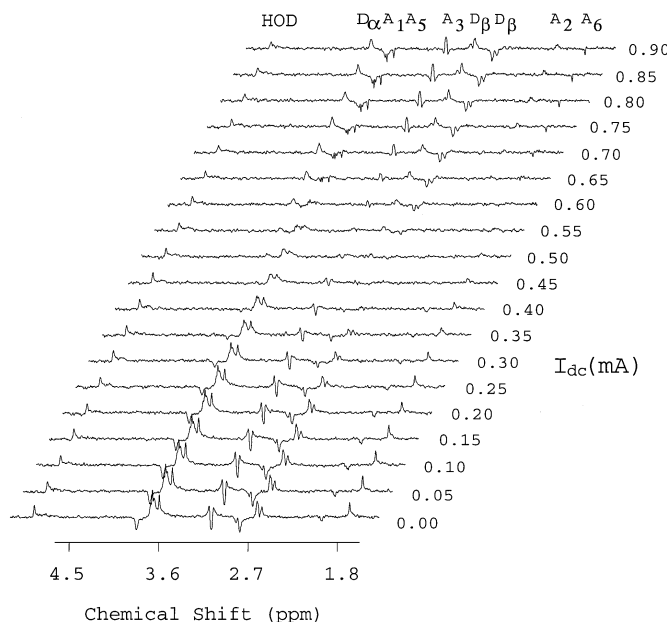
(b)

FIG. 3. (a) The control proton spin-echo ENMR spectrum and (b) the proton CC-ENMR spectrum acquired from a solution containing 100 mM L-aspartic acid (D) and 100 mM 4,9-dioxa-1,12-dodecanediamine (A) in D_2O. The solution electric conductivity (κ) was 5.30 mS $\cdot$ cm^{-1}. The pulse sequence parameters were $\Delta = 300.118$ ms, $\tau = 161.118$ ms, $\tau_D = 310.136$ ms, $t_1 = 50$ ms, NS $= 32$, $T_R = 3$ s, $g = 304.5$ mT $\cdot$ m^{-1}, $\delta = 1$ ms, and $K = 814.6$ cm^{-1}. The DC electric field has a duration of 600 ms with a stepwise amplitude increase from 0 to 34.6 V $\cdot$ cm^{-1}. The parameters of the control spectrum were $\Delta = 600.018$ ms, $\tau = 360.080$ ms, $\tau_D = 610.163$ ms, and NS $= 32$. The other experimental conditions were the same as in the CC-ENMR experiment.

However, increasing electric current leads to severe heat-induced convection because electrical power deposition ($p = I_e^2 R t$) is a quadratic function of electric current. As a result, only low conductivity sample solutions can be studied using these earlier ENMR methods (*1, 8–10, 12, 13, 23–25*). To obtain sufficient electric field and reduce the convection effect, we introduced the CA-ENMR technique using capillary array ENMR chambers (*3*). The small cross-sectional area (*A*) of the capillaries in the CA-ENMR sample tubes increases the $\frac{I_e}{A}$ ratio (or E_{dc}) at modest electric current. As a result, electrophoretic flow measurements can be carried out for solutions of high conductivity (κ). The restricted molecular motion in the bundled capillaries reduces heat-induced convection and electrical eddy current, which improves the probe *Q*-factor (*3*). Bundled capillaries, instead of a single capillary, were chosen to increase both RF coil filling factor and sample volume for an optimum signal detection sensitivity. Since capillaries are parallel to the static magnetic field, potential reduction in spectral quality due to magnetic susceptibility effect is avoided. Because cooling air flows between capillaries in the CA-ENMR configuration, heat exchange in CA-ENMR is basically the same as in the single capillary configuration. CC-ENMR utilizes these CA-ENMR features and further enhances the CA-ENMR method by removing residual convection artifacts.

CONCLUSIONS

A novel experimental method, CC-ENMR, has been developed and demonstrated to remove spectral artifacts from heat-induced convection. With an intrinsic sequence symmetry, the experiment generates a time-reversal event that refocuses spin phase distortions due to convective flow. Switching polarity of the DC electric field breaks this symmetry for charged particles to retain their phase accumulations for electrophoretic flow measurement. For samples of high ionic strength, the CA-ENMR chambers are required to establish sufficient electric field. Note that the back-to-back sequence construction strategy can also be applied for flow compensation in MRI and, conversely, that the numerous gradient waveforms developed in the flow compensated MRI sequences can be employed to suppress convection artifacts in ENMR. The combined approach of CC-ENMR and CA-ENMR removes heat-induced convection, thereby enhancing the capability of ENMR as a potentially powerful method for structural characterization of protein interactions and biological signaling processes.

REFERENCES

1. Q. He, Y. Liu, and T. Nixon, High-field electrophoretic NMR of mixed proteins in solution, *J. Am. Chem. Soc.* **120,** 1341 (1998).

2. Q. He, W. Lin, Y. Liu, and E. Li, Three-dimensional electrophoretic NMR correlation spectroscopy, *J. Magn. Reson.* **147,** 361 (2000).

3. Q. He, Y. Liu, H. Sun, and E. Li, Capillary array electrophoretic NMR of proteins in biological buffer solutions, *J. Magn. Reson.* **141,** 355 (1999).

4. J. G. Pipe and T. L. Chenevert, A progressive gradient moment nulling design technique, *Magn. Reson. Med.* **19,** 175 (1991).

5. A. Jerschow and N. Muller, Convection compensation in gradient enhanced nuclear magnetic resonance spectroscopy, *J. Magn. Reson.* **132,** 13 (1998).

6. P. J. Keller and F. W. Wehrli, Gradient moment nulling through the nth moment. application of binomial expansion coefficients to gradient amplitudes, *J. Magn. Reson.* **78,** 145 (1988).

7. J. L. Duerk and O. P. Simonetti, Review of MRI gradient waveform design methods with application in the study of motion, *Concept Magn. Reson.* **5,** 105 (1993).

8. Q. He and C. S. Johnson, Jr., Two-dimensional electrophoretic NMR for the measurement of mobilities and diffusion in mixtures, *J. Magn. Reson.* **81,** 435 (1989).

9. Q. He and C. S. Johnson, Jr., Stimulated echo electrophoretic NMR, *J. Magn. Reson.* **85,** 181 (1989).

10. Q. He, D. P. Hinton, and C. S. Johnson, Jr., Measurement of mobility distributions for vesicles by electrophoretic NMR, *J. Magn. Reson.* **91,** 654 (1991).

11. F. M. Coveney, J. H. Strange, A. L. Smith, and E. G. Smith, NMR studies of electrophoretic mobility in surfactant systems, *Colloids Surfaces* **36,** 193 (1989).

12. C. S. Johnson, Jr., and Q. He, Electrophoretic NMR, *in* "Advances in Magnetic Resonance" (W. S. Warren, Ed.), p. **131,** Academic Press, San Diego, 1989.

13. Q. He, "Electrophoretic Nuclear Magnetic Resonance," Ph.D. Thesis, University of North Carolina at Chapel Hill, 1990.

14. S. R. Heil and M. Holz, Electrical transport in a disordered medium: NMR measurement of diffusivity and electrical mobility of ionic charge carriers, *J. Magn. Reson.* **135,** 17 (1998).

15. T. R. Saarinen and C. S. Johnson, Jr., High-resolution electrophoretic NMR, *J. Am. Chem. Soc.* **110,** 3332 (1988).

16. M. Holz, D. Seiferling, and X. Mao, Design of a new electrophoretic NMR probe and its application to $^7Li^+$ and $^{133}Cs^+$ mobility studies, *J. Magn. Reson. A* **105,** 90 (1993).

17. M. Holz, Electrophoretic NMR, *Chem. Soc. Rev.* **23,** 165 (1994).

18. S. R. Heil and M. Holz, A mobility filter for the detection and identification of charged species in complex liquid mixtures by ENMR phase difference spectroscopy, *Angew. Chem. Int. Ed. Engl.* **35,** 1717 (1996).

19. M. Holz and C. Muller, NMR measurement of internal magnetic field gradients caused by the presence of an electric current in electrolyte solutions, *J. Magn. Reson.* **40,** 595 (1980).

20. M. Holz and C. Muller, Direct measurement of single ionic drift velocities in electrolyte solutions. An NMR method, *Ber. Bunsenges. Phys. Chem.* **86,** 141 (1982).

21. M. Holz, O. Lucas, and C. Muller, NMR in the presence of an electric current. Simultaneous measurements of ionic mobilities, transfer numbers, and self-diffusion coefficients using an NMR pulsed-gradient experiment, *J. Magn. Reson.* **58,** 294 (1984).

22. M. Holz, C. Muller, and A. M. Wachter, Modification of the pulsed magnetic field gradient method for the determination of low velocities by NMR, *J. Magn. Reson.* **69,** 108 (1986).

23. C. S. Johnson, Jr., Electrophoretic NMR, *in* "Encyclopedia of NMR" (D. Grant, Ed.), p. 1886, Wiley, New York (1995).

24. K. F. Morris and C. S. Johnson, Jr., Mobility-ordered 2D NMR spectroscopy for the analysis of ionic mixtures, *J. Magn. Reson. A* **100,** 67 (1993).

25. K. F. Morris and C. S. Johnson, Jr., Mobility-ordered two-dimensional nuclear magnetic resonance spectroscopy, *J. Am. Chem. Soc.* **114,** 776 (1992).

26. J. H. Strange, E. G. Smith, and F. M. Coveney, NMR apparatus and method for electrophoretic mobility, European Patent 0 361 942 A2 (1989).

27. H. Dai and T. A. Zawodzinski, Jr., Determination of lithium ion transference numbers by electrophoretic nuclear magnetic resonance, *J. Electrochem. Soc.* **143,** L107 (1996).

28. D. P. Hinton and C. S. Johnson, Jr., Diffusion coefficients, electrophoretic mobilities, and morphologies of charged phospholipid vesicles by pulsed field gradient NMR and electron microscopy, *J. Colloid Interface Sci.* **173,** 364 (1995).